ChemPubSoc Europe

DOI: 10.1002/chem.201504606

CHEMISTRY
A European Journal
Full Paper

Photocatalysts

Control of Surface Plasmon Resonance of Au/SnO_2 by Modification with Ag and Cu for Photoinduced Reactions under Visible-Light Irradiation over a Wide Range

Atsuhiro Tanaka,[a, b] Keiji Hashimoto,[a] and Hiroshi Kominami*[a]

Abstract: Gold particles supported on tin(IV) oxide (0.2 wt% Au/SnO_2) were modified with copper and silver by the multistep photodeposition method. Absorption around $\lambda =$ 550 nm, attributed to surface plasmon resonance (SPR) of Au, gradually shifted to longer wavelengths on modification with Cu and finally reached $\lambda = 620$ nm at 0.8 wt% Cu. On the other hand, the absorption shifted to shorter wavelength with increasing amount of Ag and reached $\lambda =$ 450 nm at 0.8 wt% Ag. These Cu- and Ag-modified 0.2 wt% Au/SnO_2 materials (Cu-Au/SnO_2 and Ag-Au/SnO_2) and 1.0 wt% Au/SnO_2 were used for mineralization of formic acid to carbon dioxide in aqueous suspension under irradiation with visible light from a xenon lamp and three kinds of light-emitting diodes with different wavelengths. The reaction rates for the mineralization of formic acid over these materials depend on the wavelength of light. Apparent quantum efficiencies of Cu-Au/SnO_2, Au/SnO_2, and Ag-Au/SnO_2 reached 5.5% at 625 nm, 5.8% at 525 nm, and 5.1% at 450 nm, respectively. These photocatalysts can also be used for selective oxidation of alcohols to corresponding carbonyl compounds in aqueous solution under visible-light irradiation. Broad responses to visible light in formic acid mineralization and selective alcohol oxidation were achieved when the three materials were used simultaneously.

Introduction

Titanium(IV) oxide (TiO_2) is a favorable photocatalyst because it consists of abundant elements (Ti and O) and is a stable and safe compound. However, a weakness TiO_2 as a photocatalyst is that it requires irradiation with UV light to induce photocatalytic reactions due to its relatively large bandgap (ca. 3.2 eV). Since UV light accounts for only about 5% of the total solar energy, sufficient utilization of solar energy cannot be achieved by a TiO_2 photocatalyst. Therefore, development of photocatalysts responding to visible light is an important topic from a practical point of view, because visible light accounts for about 50% of the total solar energy. Most of the visible-light-responsive photocatalysts, such as doped (or modified) TiO_2[1] and narrow-bandgap photocatalysts with a cocatalyst,[2] work under irradiation of light with wavelengths shorter than $\lambda =$ 480 nm. The development of photocatalysts that operate under irradiation of light with wavelengths longer than $\lambda =$ 480 nm is important in order to utilize solar energy efficiently.

Nanoparticles of metals such as gold, silver, and copper have been studied extensively because of their unique properties, which are associated with their strong photoabsorption in the visible light region, due to surface plasmon resonance (SPR).[3] The photoabsorption peaks due to SPR of Au, Ag, and Cu nanoparticles are generally observed around 550, 450, and 600 nm, respectively. Recently, Au nanoparticles supported on TiO_2 and cerium(IV) oxide (CeO_2) have been applied as a new type of photocatalysts responding to visible light.[4] Previously, we found that action spectra in photocatalytic reactions over Au/TiO_2 and Au/CeO_2 were in good agreement with their absorption spectra, which suggested that photocatalytic reactions were induced by photoabsorption due to SPR of the supported Au nanoparticles. In contrast to reports on supported Au nanoparticles, there have been few reports on chemical reactions induced by SPR of Ag and Cu nanoparticles, probably due to their instability under working conditions. To utilize the unique SPR property of Cu, we examined modification of CeO_2-supported Au nanoparticles with Cu and found that photoabsorption due to SPR was shifted to longer wavelength.[5] Over thus-prepared Cu-Au/CeO_2 materials, organic acids in aqueous solutions were mineralized to CO_2 even under irradiation with visible light of $\lambda = 700$ nm.[5] These results suggest that photoabsorption due to SPR of supported Au nanoparticles can be controlled by modification with Ag and Cu and that the modified metal nanoparticles show a wide response to visible light, which results in efficient utilization of solar energy.

In this study, we examined control of absorption due to SPR by modification of Au nanoparticles supported on SnO_2 with Ag and Cu. SnO_2 attracted our interest for use as a support for metal nanoparticles having photoabsorption due to SPR since

---

[a] *Dr. A. Tanaka, Dr. K. Hashimoto, Dr. H. Kominami*
Department of Applied Chemistry, Faculty of Science and Engineering
Kindai University, Kowakae, Higashiosaka, Osaka 577-8502 (Japan)
E-mail: hiro@apch.kindai.jp

[b] *Dr. A. Tanaka*
Department of Applied Chemistry, College of Life Sciences
Ritsumeikan University, 1-1-1 Noji-higashi, Kusatsu, Shiga 525-8577 (Japan)

Supporting information for this article is available on the WWW under http://dx.doi.org/10.1002/chem.201504606.

it is a wide-bandgap (3.2 eV) photocatalyst that cannot absorb visible light, the contribution of which is completely eliminated from the photoabsorption of modified samples in the range of visible light. The position of the conduction band edge of SnO_2, about 0.5 eV lower than those of TiO_2 and ZnO,[6,7] indicates that one-electron reduction of O_2, that is, formation of $O_2^{\bullet-}$ radical ($O_2 + e^- \rightarrow O_2^{\bullet-}$), does not occur. Two-electron reduction of O_2 ($O_2 + 2e^- + 2H^+ \rightarrow H_2O_2$) and four-electron reduction of O_2 ($O_2 + 4e^- + 4H^+ \rightarrow 2H_2O$) may occur. Since H_2O_2 is probably decomposed to water and O_2 over Au nanoparticles, active oxygen species would be removed from the reaction system, which also eliminates the contribution of active oxygen species to photoinduced reactions. Herein, we report 1) mineralization of formic acid and selective oxidation of alcohols in aqueous suspensions of Au/SnO_2, Ag-Au/SnO_2, and Cu-Au/SnO_2 under irradiation with visible light and 2) simultaneous use of all three materials to achieve a wide response to visible light.

Results and Discussion

TEM observations

Figure 1 shows TEM images of unmodified and modified Au/SnO_2 samples. Figure 1 a shows a TEM image of Au(0.2)/SnO_2. Au particles were observed in the TEM image and the average diameter was determined to be 3.8 nm, that is, Au nanoparticles were successfully deposited on the surface of SnO_2 by using the photodeposition (PD) method. Previously, we found that the size of Au nanoparticles loaded on CeO_2 gradually increased with repeating Au photodeposition.[8] In the multistep photodeposition (MSPD) method, the metal source is reduced and deposited as the metal on previously deposited metal particles acting as reduction sites, which results in the growth of metal particles on CeO_2 under light irradiation.

In the present study, we used MSPD for preparation of Au/SnO_2 with larger Au particles. As expected, larger particles were observed in the TEM image of Au(1.0)/SnO_2 (Figure 1 b), and the average diameter of the Au particles was determined to be 8.2 nm. This indicates that MSPD is applicable for preparation of Au/SnO_2 with larger Au particles as well as Au/CeO_2. Since MSPD has also been shown to be effective for introduction of a second metal (Cu) onto Au particles loaded on CeO_2,[5] it was used for modification of Au/SnO_2 with second metals (Ag and Cu) in this study. As shown in Figure 1 c and d, larger particles were also observed in the TEM images of Ag(0.8)-Au(0.2)/SnO_2 and Cu(0.8)-Au(0.2)/SnO_2, and the average diameters of the particles were determined to be 8.6 and 8.5 nm, respectively (Supporting Information, Figure S1). Increases in particle size after introduction of Ag and Cu clearly indicate that the second metals were deposited on the Au particles, and that MSPD is useful for preparation of supported Ag–Au and Cu–Au bimetallic materials.

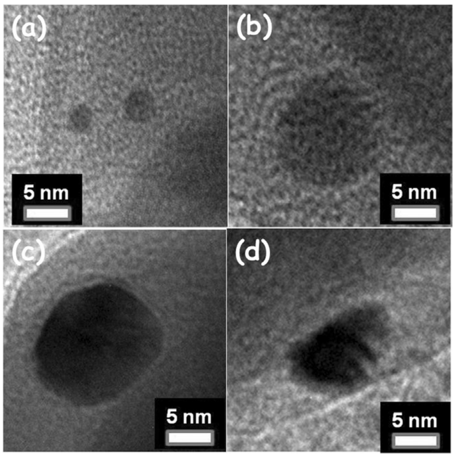

Figure 1. TEM images of a) Au(0.2)/SnO_2, b) Au(1.0)/SnO_2, c) Ag(0.8)-Au0.2)/SnO_2, and d) Cu(0.8)-Au(0.2)/SnO_2.

Photoabsorption properties

Figure 2 shows absorption spectra of Au(0.2)/SnO_2, Ag(0.8)-Au(0.2)/SnO_2, Au(1.0)/SnO_2, and Cu(0.8)-Au(0.2)/SnO_2. In the spectra of Au(0.2)/SnO_2 and Au(1.0)/SnO_2, photoabsorption was observed around $\lambda = 550$ nm (Figure 2 d, b), which was attributed to SPR of the supported Au particles,[4,5,8,9] and more intense photoabsorption was achieved by increasing the Au contents of Au/SnO_2 and Au/CeO_2.[8] Both a shift of photoabsorption and an increase in intensity were achieved by introduction of Ag and Cu into Au(0.2)/SnO_2 by MSPD (Figure 2 a, c). The photoabsorption at 550 nm of Ag(0.8)-Au(0.2)/SnO_2 and that of Cu(0.8)-Au(0.2)/SnO_2 at 550 nm were less intense than that of the Au(0.2)/SnO_2 mother material before modification. These results suggest that the SPR properties of Ag(0.8)-Au(0.2)/SnO_2 and Cu(0.8)-Au(0.2)/SnO_2 are not inherited from Au(0.2)/SnO_2 and originate from the properties of Ag and Cu themselves. In other experiments, however, we did not succeed in the preparation of Au-free Cu/SnO_2 exhibiting SPR by PD and MSPD. In addition, it is known that Cu nanoparticles

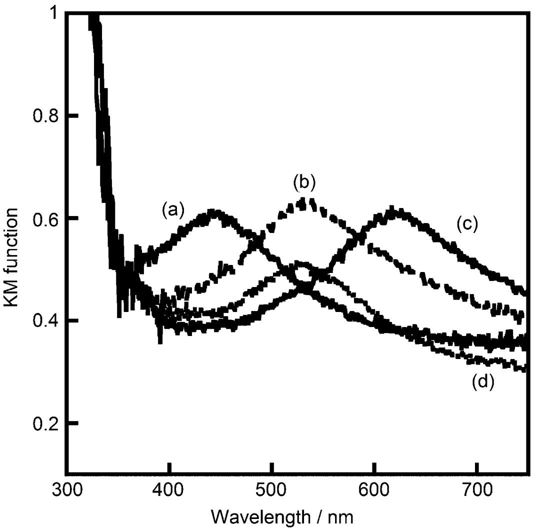

Figure 2. Absorption spectra of a) Ag(0.8)-Au(0.2)/SnO_2, b) Au(1.0)/SnO_2, c) Cu(0.8)-Au(0.2)/SnO_2, and d) Au(0.2)/SnO_2.

are easily oxidized and lose their SPR gradually under ambient conditions.[10] Therefore, Au particles are clearly indispensable for preparation of stable Cu-based particles supported on SnO_2 exhibiting intense photoabsorption at 630 nm due to SPR. The Au particles probably function as a kind of template and stabilizer for Cu and Ag metals. However, we did not observe a core–shell structure in TEM images of Ag(0.8)-Au(0.2)/SnO_2 and Cu(0.8)-Au(0.2)/SnO_2.

Figure 3 a, b shows the influence of Ag and Cu contents (*X* and *Y* wt%, respectively) in the Ag(*X*)-Au(0.2)/SnO_2 and Cu(*Y*)-Au(0.2)/SnO_2 samples on the top wavelength due to SPR λ_{top} and photoabsorption (one-reflection) at λ_{top}. The photoabsorption at λ_{top} increased with increasing Ag and Cu contents. The maximum peaks gradually shifted to shorter and longer wavelengths with increasing *X* and *Y* and reached $\lambda = 450$ nm at $X = 0.8$ wt% and $\lambda = 630$ nm at $Y = 0.8$ wt%. Thus, the peak position of photoabsorption due to SPR can be controlled by modification of Au(0.2)/SnO_2 with Ag and Cu by MSPD.

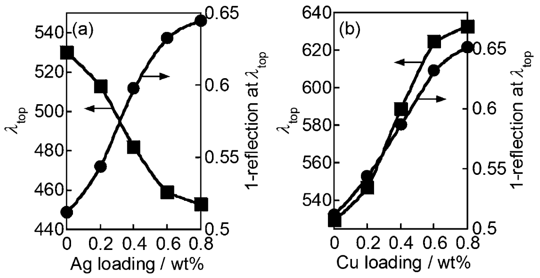

Figure 3. Influence of a) Ag loading *X* and b) Cu loading *Y* on Au(0.2)/SnO_2 on the top of the wavelength due to SPR λ_{top} and one-reflection photoabsorption at λ_{top}.

Photocatalytic mineralization of formic acid in aqueous suspensions of Au(1.0)/SnO_2, Ag(0.8)-Au(0.2)/SnO_2, and Cu(0.8)-Au(0.2)/SnO_2

Figure 4 shows time courses of evolution of CO_2 from formic acid in aqueous suspensions of Au(1.0)/SnO_2, Ag(0.8)-Au(0.2)/SnO_2, and Cu(0.8)-Au(0.2)/SnO_2 under irradiation from green, blue, and red light-emitting diodes (LEDs) with maximum wavelengths of 475, 530, and 640 nm, respectively (Figure 5). In the presence of Au(1.0)/SnO_2 (circles in Figure 4), CO_2 was evolved after irradiation with green, blue, and red lights, and CO_2 formation continued linearly with irradiation time, indicating zero-order kinetics over Au(1.0)/SnO_2.

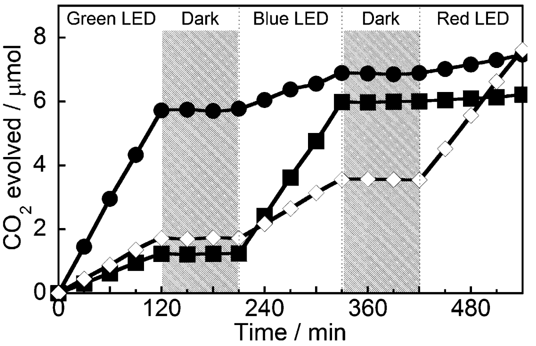

Figure 4. Time courses of evolution of CO_2 from formic acid in aqueous suspensions of Au(1.0)/SnO_2 (circles), Ag(0.8)-Au(0.2)/SnO_2 (squares), and Cu(0.8)-Au(0.2)/SnO_2 (diamonds) under irradiation with visible light from green, blue, and red LEDs (1.7 mW cm^{-2}).

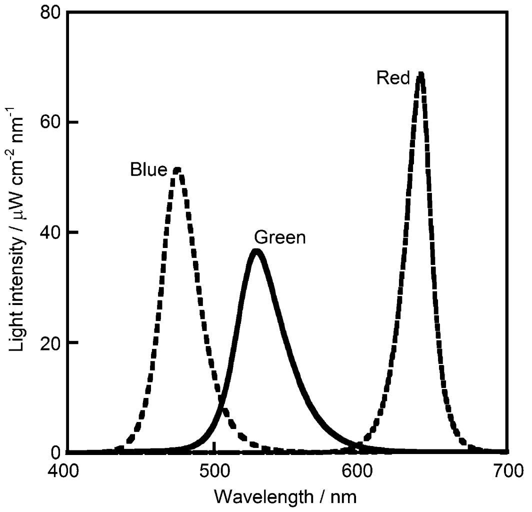

Figure 5. Spectra of visible light from blue, green, and red LEDs (1.7 mW cm^{-2}) used for photoinduced reactions.

On the other hand, the absence of gas evolution in the dark indicated that no thermocatalytic mineralization of formic acid occurred under the present conditions. From the slopes of time courses of CO_2 evolution, rates over Au(1.0)/SnO_2 under irradiation with green, blue, and red lights were determined to be 2.9, 0.55, and 0.29 μmol h^{-1}, respectively. As shown in Figures 2 b and 5, photoabsorption due to SPR of Au(1.0)/SnO_2 overlapped well with light from the green LED, and the greater utilization of light (photons) explains the highest rate under green-light irradiation. Similarly, rates of CO_2 formation over Cu(0.8)-Au(0.2)/SnO_2 (diamonds in Figure 4) under irradiation with green, blue, and red lights were determined to be 0.86, 0.93, and 2.1 μmol h^{-1}, respectively. Owing to the strong photoabsorption of Cu(0.8)-Au(0.2)/SnO_2 at 630 nm (Figure 2 c), it exhibited the highest rate under red-light irradiation. In the case of Ag(0.8)-Au(0.2)/SnO_2 (squares in Figure 4), the CO_2 formation rates under irradiation with green, blue, and red lights were determined to be 0.62, 2.4, and 0.11 μmol h^{-1}, respectively. The highest rate for Ag(0.8)-Au(0.2)/SnO_2 was obtained with blue-light irradiation, as expected from the photoabsorption properties. These results indicate that the materials exhibit the best performance under irradiation with visible light overlapping with their SPR.

The stability of Au(1.0)/SnO_2, Ag(0.8)-Au(0.2)/SnO_2, and Cu(0.8)-Au(0.2)/SnO_2 in the mineralization of formic acid was evaluated by prolonged use under irradiation with light from green, blue, and red LEDs, respectively, and all three materials continuously decomposed formic acid without losing their activity (Figure 6). After irradiation for about 50 h, CO_2 evolution was almost saturated at about 100 μmol, which corresponds to the initial amount of formic acid (100 μmol) and indicates that

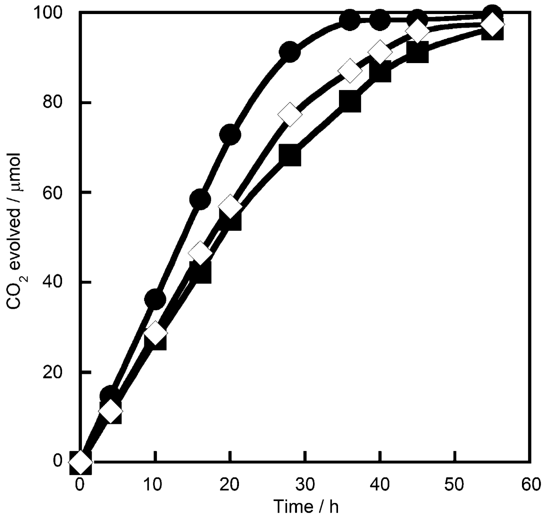

Figure 6. Time courses of evolution of CO_2 from formic acid (100 µmol) in aqueous suspensions of Au(1.0)/SnO_2 (circles), Ag(0.8)-Au(0.2)/SnO_2 (squares), and Cu(0.8)-Au(0.2)/SnO_2 (diamonds) under irradiation with visible light from green, blue and red LEDs (1.7 mW cm^{-2}), respectively.

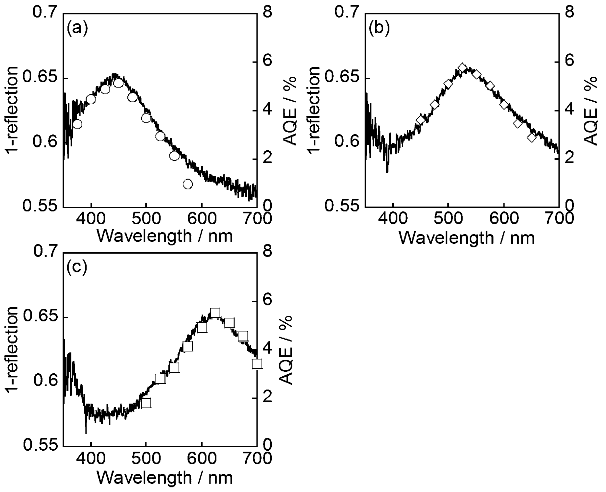

Figure 7. Absorption spectra measured with barium sulfate as a reference (left axis) and action spectra (circles) in formic acid mineralization (right axis). a) Ag(0.8)-Au(0.2)/SnO_2, b) Au(1.0)/SnO_2, and c) Cu(0.8)-Au(0.2)/SnO_2.

formic acid was almost completely decomposed to CO_2 ($HCOOH + 0.5\,O_2 \rightarrow CO_2 + H_2O$) over Au(1.0)/$SnO_2$, Au(0.2)-Ag(0.8)/$SnO_2$, and Au(0.2)-Cu(0.8)/$SnO_2$ under irradiation with green, blue, and red light, respectively. The amounts of CO_2 evolved were about fifteen times larger than the total amounts (2.5, 4.2, and 6.8 µmol, respectively) of Au, Ag-Au, and Cu-Au loaded on SnO_2, that is, mineralization of formic acid was not a quantitative reaction but a photocatalytic reaction.

Action spectra

The action spectrum is a powerful tool for determining whether an observed reaction occurs by a photoinduced or a thermocatalytic process. To obtain action spectra in this reaction system, mineralization of formic acid in aqueous suspensions of Au(1.0)/SnO_2, Ag(0.8)-Au(0.2)/SnO_2, and Cu(0.8)-Au(0.2)/SnO_2 was carried out at 298 K under irradiation with monochromated visible light from an Xe lamp with a light width of ±5 nm. The apparent quantum efficiency (AQE) at each centered wavelength of light was calculated from the ratio of the amount of CO_2 and the amount of incident photons (see Supporting Information) by using Equation (1).

$$\mathrm{AQE} = \frac{\text{amount of } CO_2}{\text{amount of incident photons}} \times 100 \qquad (1)$$

The results are shown in Figure 7. Wavelength dependences of AQEs over Au(1.0)/SnO_2, Ag(0.8)-Au(0.2)/SnO_2, and Cu(0.8)-Au(0.2)/SnO_2 were similar to those of their photoabsorption (one-reflection), and this indicates that formation of CO_2 from formic acid in aqueous suspensions of the three materials was induced by photoabsorption due to their SPR. AQEs exceeding 5% were obtained for all three materials when they were irradiated with light matching their SPR.

Selective oxidation of various substrates in aqueous suspensions of Ag(0.8)-Au(0.2)/SnO_2, Au(1.0)/SnO_2, and Cu(0.8)-Au(0.2)/SnO_2

Previously, we found almost quantitative oxidation of benzyl alcohols to benzaldehydes in an aqueous suspension of Au/CeO_2 under irradiation with green light from an LED.[8] Herein, Ag(0.8)-Au(0.2)/SnO_2, Au(1.0)/SnO_2, and Cu(0.8)-Au(0.2)/SnO_2 were used for oxidation of benzyl alcohol under irradiation with light from three LEDs to evaluate their performance in photocatalytic conversions other than mineralization. No oxidation of benzyl alcohol occurred over metal-free SnO_2; thus, visible light from the LEDs did not cause bandgap excitation of SnO_2. On the other hand, Ag(0.8)-Au(0.2)/SnO_2, Au(1.0)/SnO_2, and Cu(0.8)-Au(0.2)/SnO_2 were active in the oxidation of benzyl alcohol and yielded benzaldehyde with quite high selectivity (>99%) at greater than 99% conversion of benzyl alcohol after 20 h when blue, green, and red LEDs were used, respectively (Supporting Information, Table S1). We confirmed that a photocatalyst, irradiation with visible light, and O_2 were indispensable for oxidation of benzyl alcohol. Since the amount of benzaldehyde increased linearly with photoirradiation time of the three materials, the formation rates were determined from slopes of the time courses of benzaldehyde formation (Figure 8). The highest reaction rates were obtained when the irradiating light overlapped well with photoabsorption due to SPR, as in the case of formic acid mineralization.

The use of Ag-Au/SnO_2, Au/SnO_2 and Cu-Au/SnO_2 for selective oxidation under visible-light irradiation was extended to various water-soluble alcohols as substrates. Ag(0.8)-Au(0.2)/SnO_2, Au(1.0)/SnO_2 and Cu(0.8)-Au(0.2)/SnO_2 were also effective in oxidation of a secondary aliphatic alcohol (2-pentanol), an alicyclic alcohol (cyclohexanol), a secondary aromatic alcohol (1-phenylethanol), and a primary aromatic alcohol (2-phenylethanol) to the corresponding aldehyde or ketone with selectivities higher than 99%, which indicates that these photocata-

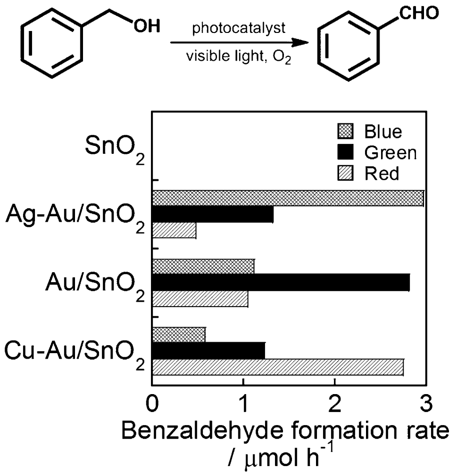

Figure 8. Rates of formation of benzaldehyde from benzyl alcohol in aqueous suspensions of SnO_2, Ag(0.8)-Au(0.2)/SnO_2, Au(1.0)/SnO_2, and Cu(0.8)-Au(0.2)/SnO_2 under irradiation with visible light from green, blue, and red LEDs (1.7 mW cm^{-2}).

Table 1. Oxidation of various alcohols in aqueous suspensions of Ag(0.8)-Au(0.2)/SnO_2 (Ag-Au), Au(1.0)/SnO_2 (Au), and Cu(0.8)-Au(0.2)/SnO_2 (Cu-Au) under irradiation with visible light from blue, green, and red LEDs in the presence of O_2.[a]

Photocatalyst	Substrate	Product	LED	t [h]	Conv.[b] [%]	Sel.[b] [%]
Ag-Au	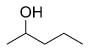	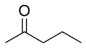	blue	32	32	>99
Au			green	32	38	>99
Cu-Au			red	32	42	>99
Ag-Au	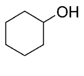	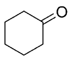	blue	30	42	>99
Au			green	30	51	>99
Cu-Au			red	30	38	>99
Ag-Au	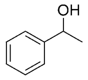	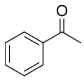	blue	48	32	>99
Au			green	48	34	>99
Cu-Au			red	48	29	>99
Ag-Au	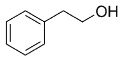	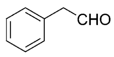	blue	68	19	>99
Au			green	68	25	>99
Cu-Au			red	68	18	>99

[a] Photocatalyst: 50 mg, substrate: 50 μmol, water: 5 cm^3, O_2: 1 atm, light intensity: 1.7 mW cm^{-2}. [b] Determined by GC with an internal standard. Conv.: conversion, Sel.: selectivity.

lysts can be used for selective oxidation of various alcohols under visible-light irradiation (See Table 1).

Photocatalytic mineralization of formic acid in aqueous solutions in the simultaneous presence of Au-Ag/SnO_2, Au/SnO_2, and Au-Cu/SnO_2

Since Au-Ag/SnO_2, Au/SnO_2, and Au-Cu/SnO_2 worked most effectively under irradiation with blue, green, and red light, respectively, we had the idea of simultaneously using these materials to effectively utilize solar light. Figure 9 shows time courses of the evolution of CO_2 from formic acid in aqueous solutions containing Au(0.2)-Ag(0.8)/SnO_2, Au(1.0)/SnO_2, and Au(0.2)-Cu(0.8)/SnO_2 (20 mg each) under irradiation with light from green, blue, and red LEDs.

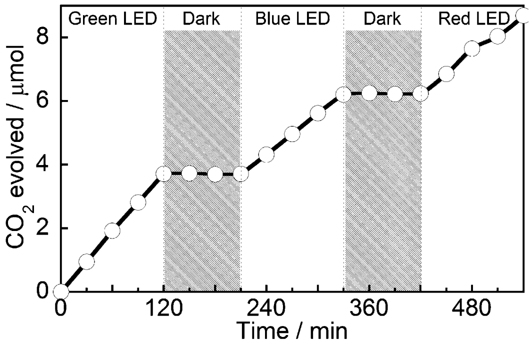

Figure 9. Time course of evolution of CO_2 from formic acid in an aqueous solution in the simultaneous presence of Ag(0.8)-Au(0.2)/SnO_2, Au(1.0)/SnO_2, and Cu(0.8)-Au(0.2)/SnO_2 under irradiation with visible light from green, blue, and red LEDs (1.7 mW cm^{-2}).

Linear evolution of CO_2 with photoirradiation was observed, and the rates under irradiation with green, blue, and red lights were determined to be 1.9, 1.3, and 1.2 μmol h^{-1}, respectively. Figure 9 also shows that no gas evolved in the dark, that is, no thermocatalytic CO_2 formation occurred under the present conditions. Figure 10 shows an action spectrum for mineralization of formic acid in an aqueous solution containing Au(0.2)-Ag(0.8)/SnO_2, Au(1.0)/SnO_2, and Au(0.2)-Cu(0.8)/SnO_2. A wide action spectrum was obtained in the presence of all three materials, and the AQE reached 3.3 % at 450 nm, 3.8 % at 550 nm, and 3.2 % at 650 nm; thus, a broad response to visible light was achieved by simultaneous use of the three materials.

Photocatalytic selective oxidation of various alcohols in aqueous solution in the simultaneous presence of Au-Ag/SnO_2, Au/SnO_2, and Au-Cu/SnO_2

Samples of all three materials (20 mg each) were simultaneously used for selective oxidation of benzyl alcohol to benzaldehyde in an aqueous solution under irradiation with visible light from an Xe lamp equipped with L-42, Y-50, and R-62 cut filters (for the resulting spectra, see Figure 11 a). The rates of benzaldehyde formation under irradiation with visible light passing through L-42, Y-50, and R-62 cut filters were 3.6, 2.6, and 1.2 μmol h^{-1}, respectively (Figure 11 b). The order L-42 > Y-50 > R-62 corresponds to the amount of photons provided to the reaction system, and this indicates that simultaneous use of three materials is effective for efficient utilization of solar light in selective oxidation of benzyl alcohol to benzaldehyde.

Applicability of the simultaneous use of three materials for photocatalytic oxidation of alcohols to the corresponding carbonyl compounds was investigated under irradiation with visible light passing through L-42, Y-50, and R-62 cut filters (Table 2). Carbonyl compounds were obtained with high selectivity (> 99 %) for all alcohols. A similar effect of cut filters on yields was observed in selective oxidation of these alcohols.

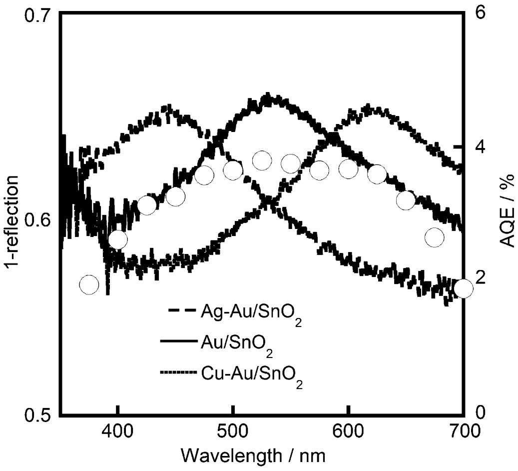

Figure 10. Absorption spectra of Ag(0.8)-Au(0.2)/SnO_2, Au(1.0)/SnO_2, and Cu(0.8)-Au(0.2)/SnO_2 measured with barium sulfate as a reference (left axis) and action spectrum in formic acid mineralization in an aqueous solution in the simultaneous presence of all three materials (right axis).

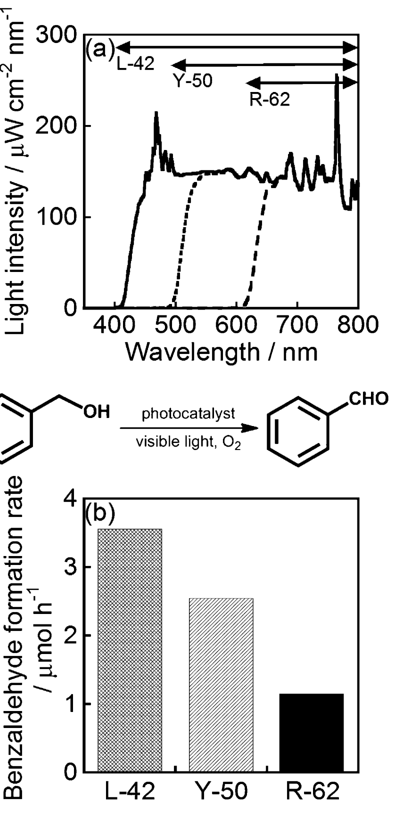

Figure 11. a) Spectra of visible light from an Xe lamp with L-42, Y-50, and R-62 cut filters. b) Rates of formation of benzaldehyde from benzyl alcohol in an aqueous solution in the simultaneous presence of Ag(0.8)-Au(0.2)/SnO_2 (Ag-Au), Au(1.0)/SnO_2, and Cu(0.8)-Au(0.2)/SnO_2 under irradiation with visible light from a Xe lamp with L-42, Y-50, and R-62 cut filters.

Proposed working mechanism

The proposed working mechanism for oxidation over plasmonic photocatalysts under irradiation with visible light is shown in Figure 12. Rapid electron transfer from SPR nanoparticles to the semiconductor film takes place under visible-light irradiation.[11] The following reaction mechanism is proposed: 1) incident photons are absorbed by metal nanoparticles through SPR excitation, 2) electrons are injected from metal nanoparticles into the conduction band of SnO_2, 3) the resultant electron-deficient metal nanoparticles could oxidize formic acid or alcohols to be returned to the original metallic state, and 4) electrons in the conduction band are consumed for reduction of oxygen. Electrons in the conduction band of SnO_2 are trapped by O_2, and H_2O_2 (two-electron reduction step) and/or H_2O (four-electron reduction step) is formed. Very high selectivity for carbonyl compounds in the present system suggests that active oxygen species were removed from the reaction system.

Table 2. Oxidation of various alcohols in aqueous solutions in the simultaneous presence of Ag(0.8)-Au(0.2)/SnO_2, Au(1.0)/SnO_2, and Cu(0.8)-Au(0.2)/SnO_2 under irradiation with visible lights from an Xe lamp with L-42, Y-50, and R-62 cut filters in the presence of O_2.[a]

Substrate	Product	Filter	t [h]	Conv.[b] [%]	Sel.[b] [%]
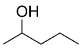	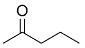	L-42	5	65	>99
		Y-50		41	>99
		R-62		25	>99
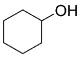	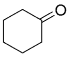	L-42	5	76	>99
		Y-50		37	>99
		R-62		21	>99
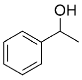	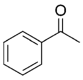	L-42	5	55	>99
		Y-50		28	>99
		R-62		12	>99
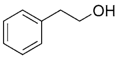	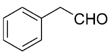	L-42	5	48	>99
		Y-50		23	>99
		R-62		9	>99

[a] Photocatalyst: 50 mg, substrate: 50 μmol, water: 5 cm^3, O_2: 1 atm, irradiation time: 5 h. [b] Determined by GC with an internal standard. Conv.: conversion, Sel.: selectivity.

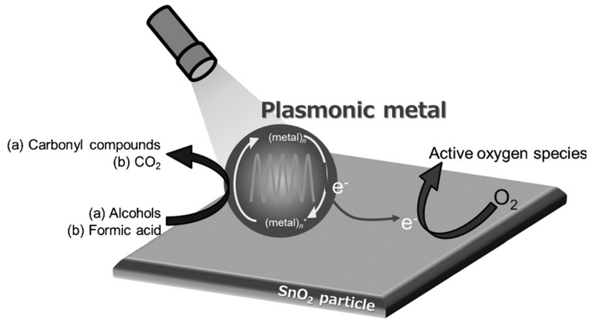

Figure 12. Proposed reaction mechanism for oxidation reactions over plasmonic metal/SnO_2 materials under irradiation with visible light.

Conclusions

SnO_2-supported Au particles exhibiting strong photoabsorption due to SPR of Au were prepared by MSPD. Modification of 0.2 wt%Au/SnO_2 with Cu and Ag by MSPD resulted in formation of Cu-Au/SnO_2 and Ag-Au/SnO_2. The absorption of the Au/SnO_2 around $\lambda = 550$ nm gradually shifted to longer and shorter wavelengths with increasing contents of Cu and Ag, respectively. Cu-Au/SnO_2 and Ag-Au/SnO_2 containing 0.8 wt% Cu and Ag showed strong absorption at around $\lambda = 450$ and 620 nm, respectively. These samples were active for mineralization of formic acid and selective oxidation of alcohols to carbonyl compounds under visible-light irradiation and exhibited the best performance when irradiated by light overlapping with their SPR. Wide responses to visible light in mineralization and selective oxidation were achieved by simultaneous use of Cu-Au/SnO_2, Au/SnO_2, and Ag-Au/SnO_2.

Experimental Section

Preparation of 0.2 wt% Au/SnO_2

Commercial SnO_2 (Nanotech, Kanto Chemical) powder was calcined at 1273 K for 1 h in a box furnace. A TEM image of the calcined SnO_2 powder is shown in Figure S1 of the Supporting Information. Gold was loaded onto SnO_2 by PD. The SnO_2 powder (198 mg) was suspended in 10 cm^3 of an aqueous solution of methanol (50 vol%) in a test tube (height: 180 mm, inner diameter: 18 mm, total volume: 35 cm^3), and the test tube was sealed with a rubber septum under argon. An aqueous solution of tetrachloroauric acid (corresponding to 0.2 wt% Au as metal, 4.0 $g\,dm^{-3}$) was injected into the sealed test tube and then photoirradiated at $\lambda > 300$ nm by a 400 W high-pressure mercury arc lamp (Eiko-sha, Osaka) with magnetic stirring in a water bath continuously kept at 298 K. The Au source was reduced by photogenerated electrons, and Au metal was deposited on the SnO_2 particles to form 0.2 wt%Au/SnO_2. The 1.0 wt% Au/SnO_2 was prepared by MSPD,[8,9] whereby PD of 0.2 wt% Au was repeated five times (1.0 wt% = 0.2 wt% × 5). These samples were designated Au(0.2)/SnO_2 and Au(1.0)/SnO_2, respectively. Analysis of the liquid phase after PD revealed that the Au source had been almost completely (>99.9%) deposited as Au metal on the SnO_2 particles. The resultant powder was washed repeatedly with distilled water and then dried in air at 310 K overnight.

Preparation of Ag-Au/SnO_2 and Cu-Au/SnO_2

MSPD was also used for preparation of Ag-Au/SnO_2 and Cu-Au/SnO_2 by modification of Au(0.2)/SnO_2 with Ag and Cu. An aqueous solution of silver sulfate (Ag: 4.0 $g\,dm^{-3}$) or copper sulfate (Cu: 4.0 $g\,dm^{-3}$) was injected into an aqueous methanolic suspension of Au(0.2)/SnO_2 and the mixture was photoirradiated with a mercury-arc lamp under the same conditions as for the preparation of Au(0.2)/SnO_2. The amount of Ag and Cu loaded per PD was fixed at 0.2 wt%, and PD of Ag and Cu was repeated for additional Ag and Cu loadings of Ag-Au(0.2)/SnO_2 and Cu-Au(0.2)/SnO_2. For example, Ag PD was repeated four times for the preparation of 0.8 wt%Ag-Au(0.2)/SnO_2. Hereafter, this material is designated Ag(0.8)-Au(0.2)/SnO_2, and that modified with 0.8 wt%Cu as Cu(0.8)-Au(0.2)/SnO_2. Analysis of the liquid phase after PD revealed that the Ag and Cu sources had been almost completely (>99.9%) deposited as Ag and Cu metals on Au(0.2)/SnO_2. The resultant powder was washed repeatedly with distilled water and then dried in air at 310 K overnight.

Characterization

Diffuse-reflectance spectra were obtained with a UV/Vvis spectrometer (UV-2400, Shimadzu, Kyoto) equipped with a diffuse-reflectance measurement unit (ISR-2000, Shimadzu). The morphology of photocatalysts was observed under a JEOL JEM-3010 transmission electron microscope operated at 300 kV in the Joint Research Center of Kindai University. LEDs (HDMS8R, Hayashi Watch Works, Tokyo) and a 500 W Xe lamp (Ushio, Tokyo) were used as light sources. Spectra and intensities of light from blue, green, and red LEDs and monochromated light from the Xe lamp were determined with a USR-45D spectroradiometer (Ushio, Tokyo).

Mineralization of formic acid in aqueous suspensions of Au/SnO_2, Ag-Au/SnO_2, and Cu-Au/SnO_2 under irradiation with visible light

Mineralization of formic acid to CO_2 over a photocatalyst under irradiation with visible light was chosen as the test reaction [Eq. (2)].[4c]

$$\mathrm{HCOOH} + 0.5\,\mathrm{O_2} \rightarrow \mathrm{CO_2} + \mathrm{H_2O} \tag{2}$$

The dried Au/SnO_2, Ag-Au/SnO_2, or Cu-Au/SnO_2 powder (50 mg) was suspended in distilled water (5 cm^3), and the suspension bubbled with O_2 and sealed with a rubber septum. Formic acid (100 μmol) was injected into the suspension, which then irradiated with visible light from a blue, green, or red LED (HDMS8B, HDMS8G, and HDMS8R, respectively, Hayashi Watch Works, Tokyo) with magnetic stirring in a water bath continuously kept at 298 K. The spectra of the visible light irradiating the reaction system is shown in Figure 5, and the maximum wavelength of the light was determined to be 475, 530, and 640 nm, respectively. The amount of CO_2 in the gas phase of the reaction mixture was measured with a gas chromatograph (GC-8A, Shimadzu) equipped with Porapak QS columns. To obtain an action spectrum, the full arc from a Xe lamp was monochromated with an SM-100 monochromator (Bunkoukeiki, Tokyo).

Oxidation of alcohols in aqueous suspensions of Au/SnO_2, Ag-Au/SnO_2, and Cu-Au/SnO_2 under irradiation with visible light

Oxidation of alcohols to carbonyl compounds (aldehydes or ketones) over photocatalysts under irradiation with visible light was chosen as test reaction.[8] The dried Au/SnO_2, Ag-Au/SnO_2, or Cu-Au/SnO_2 powder (50 mg) was suspended in distilled water (5 cm^3), and the suspension bubbled with O_2 and sealed with a rubber septum. Alcohols were injected into the suspensions, which were then irradiated with visible light from blue, green, and red LEDs. The amounts of alcohols and carbonyl compounds in the liquid phase were determined with a Shimadzu GC-14B gas chromatograph equipped with a DB-1 capillary column (30 m, 0.25 mm). The reaction solution (1 cm^3) was added to diethyl ether/water (2/1 v/v, 3 cm^3). Toluene was used as internal standard (injection amount: 100 μL, toluene/2-propanol, 50 μL/5 mL). After the mixture had been stirred for 10 min, alcohols and carbonyl compounds in the ethereal phase were analyzed. The amounts of alcohols and carbonyl compounds were determined from the ratios of the peak areas of alcohol and carbonyl compound to the peak area of toluene (see Supporting Information for details).

Acknowledgements

This work was partly supported by JSPS KAKENHI Grant Numbers 26289307, 26630415, and 15K18269. This work was also supported by MEXT-Supported Program for the Strategic Research Foundation at Private Universities 2014–2018, subsidy from MEXT and Kindai University. H.K. is grateful for financial support from the Faculty of Science and Engineering, Kindai University.

Keywords: gold · nanoparticles · photochemistry · supported catalysts · surface plasmon resonance

[1] a) R. Asahi, T. Morikawa, T. Ohwaki, K. Aoki, Y. Taga, *Science* **2001**, *293*, 269 – 271; b) H. Kisch, L. Zang, C. Lange, W. F. Maier, C. Antonius, D. Meissner, *Angew. Chem. Int. Ed.* **1998**, *37*, 3034 – 3036; *Angew. Chem.* **1998**, *110*, 3201 – 3203; c) T. Ohno, M. Akiyoshi, T. Umebayashi, K. Asai, T. Mitsui, M. Matsumura, *Appl. Catal. A* **2004**, *265*, 115 – 121; d) S. Kitano, K. Hashimoto, H. Kominami, *Appl. Catal. B* **2011**, *101*, 206 – 211.

[2] a) R. Abe, H. Takami, N. Murakami, B. Ohtani, *J. Am. Chem. Soc.* **2008**, *130*, 7780 – 7781; b) T. Arai, M. Horiguchi, M. Yanagida, T. Gunji, H. Sugihara, K. Sayama, *Chem. Commun.* **2008**, 5565 – 5567; c) A. Tanaka, K. Hashimoto, H. Kominami, *Chem. Lett.* **2011**, *40*, 354 – 356; d) Y. Sasaki, A. Tanaka, K. Hashimoto, H. Kominami, *Chem. Lett.* **2013**, *42*, 419 – 421.

[3] M. A. Garcia, *J. Phys. D* **2011**, *44*, 283001 – 283020.

[4] a) E. Kowalska, R. Abe, B. Ohtani, *Chem. Commun.* **2009**, 241 – 243; b) E. Kowalska, O. O. P. Mahaney, R. Abe, B. Ohtani, *Phys. Chem. Chem. Phys.* **2010**, *12*, 2344 – 2355; c) H. Kominami, A. Tanaka, K. Hashimoto, *Chem. Commun.* **2010**, *46*, 1287 – 1289; d) X. Zhou, G. Liu, J. Yu, W. Fan, *J. Mater. Chem.* **2012**, *22*, 21337 – 21354; e) S. Linic, P. Christopher, D. B. Ingram, *Nat. Mater.* **2011**, *10*, 911 – 921; f) C. Wang, D. Astruc, *Chem. Soc. Rev.* **2014**, *43*, 7188 – 7216; g) Q. Xiao, E. Jaatinen, H. Zhu, *Chem. Asian J.* **2014**, *9*, 3046 – 3064.

[5] A. Tanaka, K. Hashimoto, H. Kominami, *ChemCatChem* **2011**, *3*, 1619 – 1623.

[6] Z. Sun, M. Liang, J. Chen, *Acc. Chem. Res.* **2015**, *48*, 1541 – 1550.

[7] P. Docampo, P. Tiwana, N. Sakai, H. Miura, L. Herz, T. Murakami, H. J. Snaith, *J. Phys. Chem. C* **2012**, *116*, 22840 – 22846.

[8] A. Tanaka, K. Hashimoto, H. Kominami, *J. Am. Chem. Soc.* **2012**, *134*, 14526 – 14533.

[9] a) A. Tanaka, S. Sakaguchi, K. Hashimoto, H. Kominami, *Catal. Sci. Technol.* **2012**, *2*, 907 – 909; b) A. Tanaka, S. Sakaguchi, K. Hashimoto, H. Kominami, *Catal. Sci. Technol.* **2014**, *4*, 1931 – 1938.

[10] a) I. Pastoriza-Santos, A. Sánchez-Iglesias, B. Rodríguez-González, Liz-L. M. Marzán, *Small* **2009**, *5*, 440 – 443; b) P. Kanninen, C. Johans, J. Merta, K. Kontturi, *J. Colloid Interface Sci.* **2008**, *318*, 88 – 95.

[11] A. Furube, L. Du, K. Hara, R. Katoh, M. Tachiya, *J. Am. Chem. Soc.* **2007**, *129*, 14852 – 14853.

Received: November 16, 2016